RJC

RASĀYAN *J. Chem.*
158-166| Special Issue | 2022
ISSN: 0974-1496 | e-ISSN: 0976-0083 | CODEN: RJCABP
http://www.rasayanjournal.com
http://www.rasayanjournal.co.in

STRUCTURE-BASED DESIGN THROUGH MOLECULAR DYNAMICS APPROACHES OF THE SMALL-MOLECULE BIOACTIVE COMPOUNDS IN CINNAMON AS INTERLEUKIN-6 (IL-6) INHIBITORS

M. M. Damayanti [1,✉], M. Rachmawati [1], E. Widiyastuti [1], Y. Kharisma[1], T. M. Fakih[2], A. Arfan[3] and D.S.F. Ramadhan[4]

[1]Department of Pathology Anatomy, Faculty of Medicine, Universitas Islam Bandung, Indonesia, 40116

[2]Department of Pharmacy, Faculty of Mathematics and Natural Sciences, Universitas Islam Bandung, Bandung, Indonesia, 40116

[3]Faculty of Pharmacy, Universitas Halu Oleo, Kendari, Indonesia, 93561.

[4]Department of Pharmacy, Poltekkes Kemenkes Makassar, Makassar, Indonesia, 90223

✉Corresponding Author: meta_md@unisba.ac.id

ABSTRACT

The lip mucosa's wound healing process necessitates using a material that can reduce inflammation, prevent infection, expedite wound closure, and inhibit scar formation. Interleukin-6 (IL-6) is a crucial modulator of the wound-healing process. Cinnamon is a natural resource with various chemical compounds and pharmacological activities, including wound healing mediated by proinflammatory cytokines such as IL-6. This research aims to identify the lead compounds for IL-6 from Cinnamon based on binding affinity, mode interaction, and stability utilizing molecular docking and dynamics. After categorizing variables such as binding energy and molecular interactions, including hydrogen bonding and hydrophobic interactions, the docking process revealed the potential of the Epicatechin, Catechin, Coumarinic acid, 1,4-benzene dicarboxylic acid, 3,4-dihydroxybenzaldehyde, and Coumarin to interact with IL-6 binding pocket. Furthermore, the stability of these compounds was assessed during a 200 ns simulation, offering satisfactory results with similar profiles based on RMSD, RMSF, SASA, Rg, and intramolecular and intermolecular hydrogen bond parameters. Catechin, Coumarin, and Epicatechin are the most potential candidates based on their affinities calculated by the MM-PBSA approach of -56.847 kJ/mol, -42.573 kJ/mol, and -38.246 kJ/mol, respectively. These are preliminary findings that may be appropriate for additional experimental investigation.

Keywords: Cinnamon, Inflammation, Interleukin-6, Molecular Docking, Molecular Dynamics.

RASĀYAN *J. Chem.*, Special Issue, 2022

This manuscript is focusing **SDG-9:** Industry, Innovation, and Infrastructure

INTRODUCTION

Immune system and dermal cell interactions play a complex role in wound healing. In the typical stages of wound healing, each kind of cell transmits signals during hemostasis, inflammation, proliferation, and remodeling.[1] The activation of neutrophils and macrophages during inflammation, which is the first step of wound healing, results in the release of mediators both pro- and anti-inflammatory.[2,3] Pro-inflammatory cytokines such as interleukin-6 (IL-6) are recognized as markers of inflammation.[4] IL-6 is one of the critical elements in the clinical and biological acute phase response to inflammation.[5] It was first observed that IL-6, a glycoprotein with a molecular weight of 26 kDa, was a non-antigen-specific B cell differentiation factor. Four cysteine residues, two N-glycosylation sites, and 184 amino acids make up IL-6.[6] Recent studies have shown that IL-6 is responsible for inflammatory disease by influencing the growth and balance of T helper 17 and regulatory T cells.[7] IL-6 functions via two separate signaling pathways, only one of which is explicitly activated during inflammation; both pathways have a wide variety of effects and impact various physiological processes even when inflammation is not present.[8] Therapeutic approaches focused on disrupting cytokine signaling networks have emerged as important therapeutic alternatives for the treatment of inflammatory, autoimmune, and cancer illnesses. It is critical to recognize that cytokines play

http://doi.org/10.31788/RJC.2022.1558192

critical roles in host defense and tissue homeostasis maintenance; nevertheless, aberrant, or excessive cytokine production impairs these activities, resulting in inflammation and tissue damage. This has resulted in the creation of novel therapeutic procedures for the treatment of many diseases that employ regulatory cytokines or, more typically, cytokine-targeted biologics.[9] This study aims to identify the lead compounds for IL-6 from Cinnamon based on binding affinity, mode interaction, and stability utilizing molecular docking and dynamics.

EXPERIMENTAL

Preparation of Ligands and Target Molecule

In this study, the target molecule was the crystal structure of human interleukin-6. The receptor structure was obtained using the access code 1ALU from the Protein Data Bank (https://www.rcsb.org/). The target molecule was prepared by eliminating water molecules and unnecessary ligands, then a polar hydrogen atom and a Kollman charge were added to the target. Based on the results of our previous study, a total of 24 compounds were collected through the Pubchem website (https://pubchem.ncbi.nlm.nih.gov/) based on the potential effects of cinnamon on health.[10] After adding a Gasteiger charge, the compounds were allowed to rotate. All these processes were performed by utilizing the Autodock Tools 1.5.6 software.[11]

Molecular Docking Procedure

The docking procedure was carried out with the assistance of the AutoDock Tools 1.5.6 program.[12] The binding sites are positioned on the x, y, and z axes with coordinates -7.677, -12.743, and 0.048, respectively, based on the location of tartaric acid as the native ligand. The docking parameter employs the Genetic Algorithm, which is run up to 100 times. The population was set to 150, and the maximum number of evaluations was 2,500,000. Each molecule's interactions are then depicted using the Discovery Studio Visualizer software.

Molecular Dynamics Procedure

The hit compound was simulated through 200 ns of molecular dynamics production (2-fs timestep). The AMBER99SB-ILDN force field was used in the simulation process, which was run using Gromacs 2016.3.[13] ACPYPE was used to generate the ligand topology and parameters.[14] The Ewald particle mesh model was used to predict electrostatic force.[15] In the solvation system, the neutralization process used the TIP3P water cube model and involved introducing Na and Cl ions. The system is heated to 310 K to maintain consistent pressure, as part of the simulation preparation process. The durability of the hydrogen bond was then assessed using assessments of its occupancy, the radius of gyration (Rg), the root-mean-square deviation and fluctuation (RMSD and RMSF), and the solvent-accessible surface area (SASA).

Detection Method

Binding Free Energy Calculation

Using the g mmpbsa package, the binding free energy of the systems was computed using the Molecular Mechanics Poisson-Boltzmann Surface Area (MM/PBSA) approach, incorporated in Gromacs 2016.3.[16] On a 0.5 grid, The Poisson-Boltzmann equation was used to compute polar desolvation energy. To simulate water solvent's dielectric constant was set at 80. The solvent's accessible surface area was multiplied by 1.4 to get the nonpolar contribution. A protein-ligand complex's binding free energy was determined using 50 snapshots obtained throughout the simulation of the system's paths.[17-19]

RESULTS AND DISCUSSION

Molecular Docking Result

Molecular docking was used to predict how the ligand and receptor would interact during binding, and the interaction was then assessed using each compound's conformational characteristics. Tartaric acid as the reference ligand was docked to the protein binding site of the 1AUL model to validate the docking procedure. The docking approach was considered credible if the root-mean-square deviation (RMSD) of the overlapping poses between the crystal structure and docking was less than 2.0 Å.

The allowable RMSD of tartaric acid between the docked and crystal structures was 2.01. A lower RMSD indicates closer proximity between the re-docking and crystallographic ligands. The estimated inhibition constant for tartaric acid is 471.23 μM, and the free energy of binding for tartaric acid is -4.54 kcal/mol. A molecule's capacity to interact with the target protein was described by its binding energy. The increasingly

negative binding energy value indicates the strong affinity of the compound to the receptor. Three hydrogen bonds (H-bond) involving the amino acid residues Gln175, Arg179, and Arg182 were discovered due to the interaction between tartaric acid and the 1ALU protein collected from the RCSB protein. Interestingly, this ligand did not show any hydrophobic interaction with the binding pocket of human interleukin-6.

Table-1: Binding Free Energy Prediction from the Chemical Constituent in Cinnamon Against IL-6

Compounds	Binding Energy (kcal/mol)	Inhibition Constant (μM)
Natural ligand (re-docking)	-4.54	471.23
Epicatechin	-5.44	103.13
Catechin	-5.27	137.3
Coumarinic acid	-5.16	164
1,4-benzenedicarboxylic acid	-5.11	179.89
3,4-dihydroxybenzaldehyde	-5.1	181.65
Coumarin	-5.09	187.23
Procyanidin B2	-4.86	274.58
Limonene	-4.84	282.04
Cinnamic acid	-4.79	309.33
Camphor	-4.74	338.12
Caffeic acid	-4.71	354.49
Cinnamylacetate	-4.69	366.98
Methyleugenol	-4.69	365.53
Terpineol	-4.68	369.92
1,8-cineole	-4.64	394.84
Eugenol	-4.38	611.92
Cinnamaldehyde	-4.11	976.28
α-pinene	-4.11	969.59
L(−)-carnitine	-4.05	1010
Cinnamyl alcohol	-4.04	1100
Protocatechuic acid glucose	-3.98	1200
9-octadecenoic acid	-3.97	1240
Linalool	-3.71	1920
Citric acid	-3.04	5900

Six cinnamon compounds were found to be top hits indicating their ability to bind interleukin-6 based on more negative binding energy than the reference ligand. The more negative binding energy values are associated with lower Ki and correlated with lower concentrations of compounds required for inhibition. Epicatechin, catechin, coumarinic acid, 1,4-benzenedicarboxylic acid, 3,4-dihydroxybenzaldehyde, and coumarin from this plant were estimated to have binding energies of -5.44, -5.27, -5.16, -5.11, -5.1, and -5.09 kcal/mol, respectively. Interestingly, H-bond interactions with Asp26 and Arg30 were always present in epicatechin, 1,4-benzenedicarboxylic acid, and 3,4-dihydroxybenzaldehyde. In addition, this compound also binds to residues Arg179 and Arg182, forming H-bond interactions with the IL-6 binding pocket except epicatechin to Gln175 residues. Meanwhile, the unique H-bond interactions were observed in catechins (Asp34 and Gln175), Coumarinic acid (Asp26, Lys129, and Leu181), and coumarins (Met67).

Molecular Dynamics Result

RMSD and RMSF Analysis

The six top-hit molecules from the molecular docking process were carried over to the 200-ns molecular dynamics simulation (MDS). The system stability was examined based on the RMSD and RMSF to determine the stability of the complexes for each chemical. Using MDS trajectory, the RMSD of the entire complex system was calculated, and the resulting graph is shown in Fig.-2A. In the initial 30-ns simulation, the system complexes quickly attained stability. Throughout the 200-ns simulation, each hit compound-IL-6 complex remained stable. 3,4-dihydroxybenzaldehyde and catechin were shown to fluctuate more than the other hit chemicals in the 180-ns period up to the simulation's conclusion, with the average RMSD value of 0.218 Å and 0.229 Å, respectively Meanwhile, the Epicatechin complex and 1,4-benzenedicarboxylic

acid showed a similar RMSD trend with an average value of 0.213 nm, followed by Coumarin with a value of 0.214 nm. Interestingly, among all the compounds in cinnamon, the Coumarinic acid complex with IL-6 was observed to be very stable, with an average RMSD value of 0.211 nm.

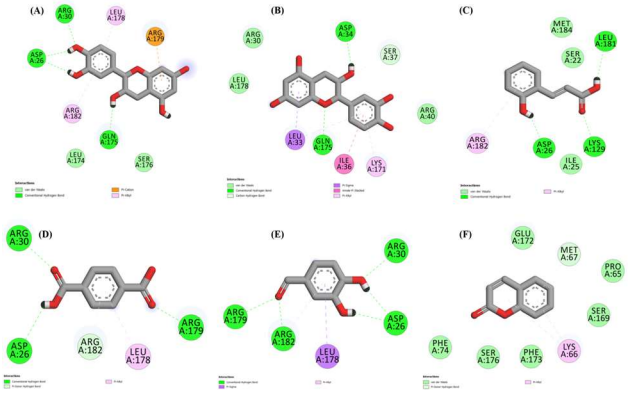

Fig.-1: The interaction of the Best Compounds of Cinnamon with IL-6, where (A) Epicatechin, (B) Catechin, (C), Coumarinic Acid, (D) 1,4-benzenedicarboxylic Acid, (E) 3,4-dihydroxybenzaldehyde, and (F) Coumarins

These results clearly show that the best-hit compound can stabilize the IL-6 system, characterized by a similar trend of RMSD fluctuations during simulation. During the simulation, each complex's RMSF value was kept track of (Fig.-2B). The amino acid variation of IL-6 over the course of 200 ns is depicted on the RMSF graph. Overall, variable amino acid residues were a common tendency across all complexes. High-intensity oscillations were observed in the Leu19, Res41, Res53, and Res124 residues. These analyses showed that the best-hit compounds did not affect the amino acid residue movement of IL-6.

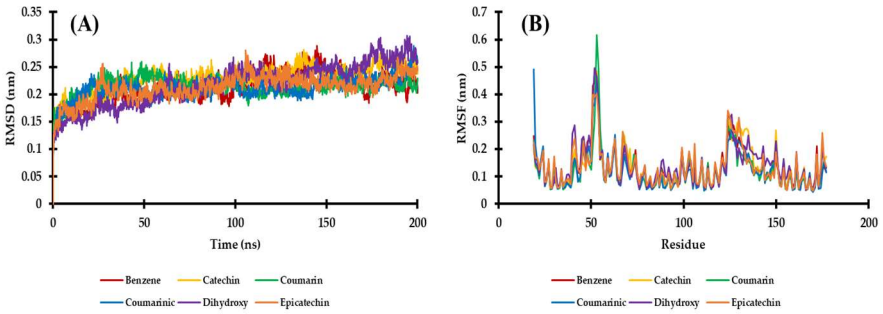

Fig.-2: Evaluation of (A) RMSD, and (B) RMSF Graph During 200 ns MD Simulations

Radius Gyration, SASA, RDF, and Hydrogen Bond Analysis

The measurement of Rg was utilized to examine the complex's stability, which was revealed by the protein folding during the simulation. The plot of Rg has presented in Fig.-3A. The molecule that was most stable in the combination with IL-6 had the lowest Rg value. It was observed that the best-hit compound had the same protein folding stability during the simulation. Based on the analysis results, the average Rg values of the epicatechin, 1,4-benzenedicarboxylic acid, Coumarinic acid, Catechin, Coumarin, and 3,4-dihydroxybenzaldehyde complexes were 1.614 nm, 1.612 nm, 1.612 nm, 1.611 nm, 1.610 nm, and 1.608 nm, respectively. The 3,4-dihydroxybenzaldehyde-IL-6 combination has the lowest Rg value, according to these findings, and is more cohesive than other hit compounds. SASA study was performed for each ligand to finish the stability assessment of each hit compound complex. These parameters can characterize the complex's folding and stability when the protein solvent area changes in simulation (Fig.-3B). The ligand-receptor complex is more stable the lower the SASA value. The graph demonstrates that all of the hit compounds provide an equally large variety of places that solvent molecules can reach. The mean SASA values for the complexes of coumarin, 3,4-dihydroxybenzaldehyde, 1,4-benzenedicarboxylic acid, catechin, epicatechin, and coumarinic acid were 92.954 nm, 93.631 nm, 93.794 nm, 93.961 nm, 94.943 nm, and 95.602 nm. Unfolded protein is known to be induced by the epicatechin and coumarinic acid complexes, which expands the region that the solvent may reach. The other complexes, however, are more stable as

evidenced by the fact that they did not noticeably change in size throughout the trial. Hydrogen bonding was required for proteins to maintain their structural conformation. The system's stability can be analyzed based on the formation of intramolecular hydrogen bonds between IL-6 and the best-hit compounds (Fig.-3C). The estimated average hydrogen bonds in Coumarin, 3,4-dihydroxybenzaldehyde, and Epicatechin were 130, respectively, while in Coumarinic acid and 1,4-benzenedicarboxylic acid complexes with IL-6 were 132. Changes in the number of hydrogen bonds in IL-6 when complexing with compounds in cinnamon are likely due to reduced ligand occupancy of the intramolecular space in the IL-6 binding pocket. The binding of the best-hit compounds from this plant can inhibit the formation of intramolecular hydrogen bonds in IL-6. However, the plot demonstrates that the complex system can maintain the structural conformation of IL-6 during the simulation, as seen by no substantial change in the number of hydrogen bonds.

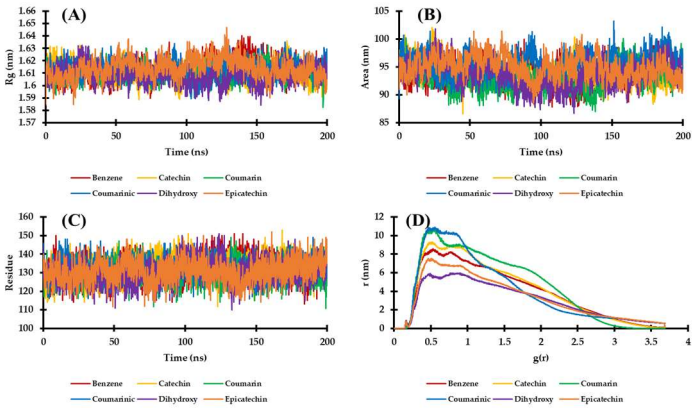

Fig.-3: Evaluation of (A) Rg, (B) SASA, (C) Intramolecular Hydrogen Bond, and (D) RDF Graph During 200ns MD Simulations

Intermolecular hydrogen bonds are essential for protein-ligand complex binding and stability. The intermolecular hydrogen bonds can describe the strength of the ligand interaction with the protein's active site. The hydrogen bonds formed between the best-hit compounds in cinnamon and IL-6 were recorded during the simulation (Fig.-4).

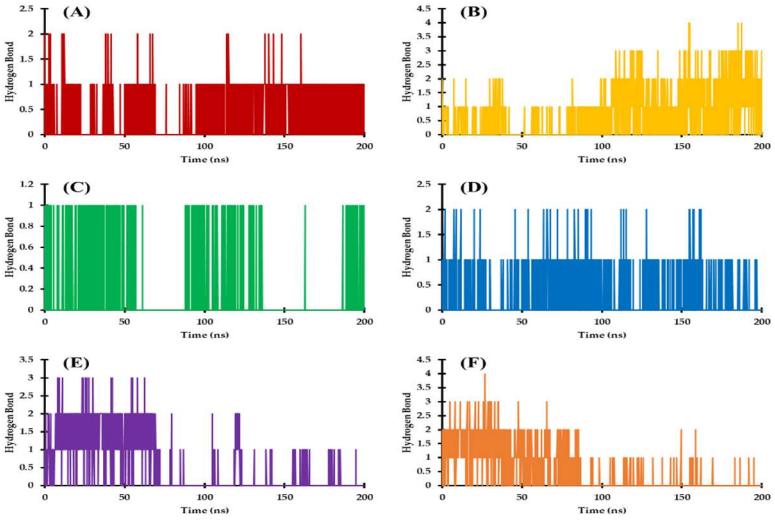

Fig.-4: Evaluation of the Intermolecular Hydrogen Bonding Interactions of the Best Compounds with IL-6. Whereas (A) 1,4-benzenedicarboxylic Acid, (B) Catechin, (C) Coumarin, (D) Coumarinic Acid, (E) 3,4-dihydroxybenzaldehyde, and (F) Epicatechin

The findings revealed the formation of up to four hydrogen bonds. The lowest hydrogen bonds were observed in the coumarin complex with one bond, followed by 1,4-benzenedicarboxylic acid and Coumarinic Acid with two bonds, 3,4-dihydroxybenzaldehyde with three bonds, and in Epicatechin and

Catechin with four hydrogen bonds. Unfortunately, the number of hydrogen bonds in the 3,4-dihydroxybenzaldehyde and Epicatechin complexes decreased over the simulation. Furthermore, the number of hydrogen bonds increased in the catechin complex, which was in line with the prediction of binding energies with the MM-PBSA method to be more negative than other compounds. This research also demonstrates intermolecular hydrogen bonds' role in forming a stable complex.

The Protein-Ligand Interaction Analysis

The hydrogen bond occupancy (H-Bonds) was also investigated during the simulation of protein-ligand interactions. H-bond occupancy with an intensity of more than 10% was observed in each complex system. One H-bond interaction with residues Met67 and Ser118 was recorded in the Coumarin and 1,4-benzenedicarboxylic acid complexes, with intensities of 11.14% and 27.87%, respectively. Interestingly, the catechin has several H-bond interactions with similar intensity to Ser37, Glu51, and Thr43 residues of 14.84%, 13.74%, and 11.64%, respectively. High-intensity H-Bond occupancy was observed in the Coumarinic Acid (25.42%), Epicatechin (45.95%), and 3,4-dihydroxybenzaldehyde (51.50%). These three compounds uniquely formed H-bonds with the same residue, Asp26, from the IL-6 binding pocket. Based on the docking results, interactions with these residues were also observed to be present.

Binding Energy Prediction with MM-PBSA Method

We continue the investigation by estimating the binding free energy of each hit complex system against IL-6 using the MM-PBSA method. Furthermore, the energy of each best compound complexed with IL-6 was compared to discover the compound with the lowest affinity energy. Table-2 provides each compound's component energies and total binding free energies. The results in Table-2 show that the van der Waals, electrostatic, and non-polar desolvation energy in the complex system was expected for ligand binding to proteins with negative values. On the other hand, the polar desolvation energy has a positive value, which is less favourable for the system. The total binding energy (ΔG_{Bind}) of the hit compound was -12.754 kJ/mol for Coumarinic Acid, -20.371 kJ/mol for 3,4-dihydroxybenzaldehyde, −31.043 kJ/mol for 1,4-benzenedicarboxylic acid, −38.246 kJ/mol for Epicatechin, -42.573 kJ/mol for Coumarin, and -56.847 kJ/mol for Catechin. These results revealed that catechins had the best potential affinity for binding to IL-6 compared to other compounds. In addition, Catechin's van der Waals energy is very favorable, with a negative contribution of -114.081 kJ/mol. This result contrasts with the polar desolvation energy, which has a positive value of -139.481 kJ/mol and weakens the system's binding energy. Furthermore, catechins have more hydrogen bond occupancy than other compounds, which could be one of the reasons for their increasingly negative binding energy.

Table-2: MM-PBSA Energy Overview from Cinnamon's Best Compounds Towards IL-6

Complex Systems	ΔEvdw (kJ/mol)	ΔEele (kJ/mol)	ΔGPB (kJ/mol)	ΔGNP (kJ/mol)	ΔGBind (kJ/mol)
IL6 + 1,4-benzenedicarboxylic acid	−64.141	−36.948	77.797	−7.751	−31.043
IL6 + Catechin	−114.081	−69.332	139.481	−12.915	−56.847
IL6 + Coumarin	−82.214	−12.380	60.268	−8.247	−42.573
IL6 + Coumarinic Acid	−77.027	−42.118	115.171	−8.781	−12.754
IL6 + 3,4-dihydroxybenzaldehyde	−29.832	−46.287	60.940	−5.192	−20.371
IL6 + Epicatechin	−87.928	−80.935	141.697	−11.081	−38.246

Note: ΔEvdw = van der Waals contribution, ΔEele = electrostatic contribution, ΔGPB = polar desolvation contribution,, ΔGNP = non-polar desolvation contribution

The present study found the estimated average hydrogen bonds in Coumarin, 3,4-dihydroxybenzaldehyde, and Epicatechin were 130, respectively, while in Coumarinic acid and 1,4-benzenedicarboxylic acid complexes with IL-6 were 132. Changes in the number of hydrogen bonds in IL-6 when complexing with compounds in cinnamon are likely due to reduced ligand occupancy of the intramolecular space in the IL-6 binding pocket. The binding of the best-hit compounds from this plant can inhibit the formation of intramolecular hydrogen bonds in IL-6. However, the plot demonstrates that the complex system can maintain the structural conformation of IL-6 during the simulation, as seen by no substantial change in the number of hydrogen bonds. Cinnamon is a medicinal plant that has long been developed. Consumption of medicinal plants has a potential role in drug development and is particularly beneficial against a variety of

human disorders.[20] Cinnamon is a medicinal plant that has long been developed. Consumption of medicinal plants has a potential role in drug development and is highly beneficial against various human disorders. 22 Studies using cinnamate as the active substance demonstrated the polymerization of polyacetylene containing cinnamic acid and its derivatives resulting in high yields of the corresponding polymer, following these events. dimerization. Cinnamic (3-phenylpropenoic) natural acid compounds and derivatives are thought to function physiologically by regulating and supporting plant development during the lignification and Suber processes.[21-24] Cinnamon contains the active compound coumarin. Research carried out in analyzing coumarins as valuable scaffolds for medicinal chemists suggests that they have unique physicochemical properties and simple and versatile synthetic transformations into a variety of functionalized coumarins as a result, a significant number of coumarin derivatives have been developed, produced, and evaluated to treat a variety of pharmacological targets selectively. An understudied secondary metabolite in the Orchidaceae family is coumarins. The 2H-chromen-2-one ring's planar, aromatic, and lipophilic properties enable improved interaction with several protein targets with a variety of pharmacological activities.[25-29] DATS inhibits naphthalene-induced oxidative damage and decreases inflammatory responses like TNF-, IL-6, IL-8, and nuclear factor-kappa B (NF-B). DATS also prevents the production of myeloperoxidase and serum nitric oxide (NO) (MPO). The anti-inflammatory cytokine interleukin-10 can be elevated by 6-gingerol while the expression of monocyte chemotactic protein-1, TNF-, interleukin-1, and interleukin-6 is decreased. In a concentration-dependent manner, lupeol inhibits macrophage osteoclastogenesis activation and production. They temporarily increase the production of p38 mitogen-activated protein kinase while decreasing the synthesis of pro-inflammatory cytokines (IL-6) (MAPK).[30-32] The findings revealed the formation of up to four hydrogen bonds. The lowest hydrogen bonds were observed in the coumarin complex with one bond, followed by 1,4-benzenedicarboxylic acid and Coumarinic Acid with two bonds, 3,4-dihydroxybenzaldehyde with three bonds, and in Epicatechin and Catechin with four hydrogen bonds. Unfortunately, the number of hydrogen bonds in the 3,4-dihydroxybenzaldehyde and Epicatechin complexes decreased over the simulation. Furthermore, the number of hydrogen bonds increased in the catechin complex, which was in line with the prediction of binding energies with the MM-PBSA method to be more negative than other compounds. This research also demonstrates intermolecular hydrogen bonds' role in forming a stable complex.

CONCLUSION

This study successfully discovered Catechin, Coumarin, and Epicatechin from Cinnamon as having IL-6 inhibitory activity, which plays a role in wound healing. These compounds had high-affinity energy estimates from docking and MM/PBSA investigations and could stabilize IL-6 during molecular dynamics simulations. This study may provide impetus to evaluate the activity of these molecules as IL-6 inhibitors experimentally.

ACKNOWLEDGMENTS

This research was supported, in part, by the Faculty of Medicine, Universitas Islam Bandung, Indonesia.

CONFLICT OF INTERESTS

The authors declare that they have no conflicts of interest about the subject matter of this article.

AUTHOR CONTRIBUTIONS

All the authors contributed significantly to this manuscript, participated in reviewing/editing, and approved the final draft for publication. The research profile of the authors can be verified from their ORCID ids, given below:

M.M.Damayanti https://orcid.org/0000-0001-8973-5772
M.Rachmawati https://orcid.org/0000-0002-8100-7663
E.Widiyastuti https://orcid.org/0000-0002-9499-7547
Y.Kharisma https://orcid.org/0000-0003-2303-0897
T.M.Fakih https://orcid.org/0000-0001-7155-4412
A.Arfan https://orcid.org/0000-0003-3004-7101
D.S.F.Ramadhan https://orcid.org/0000-0001-6257-7276

REFERENCES

1. S. Ellis, E. J. Lin, and D. Tartar, *Current Dermatoogyl Reports*, **7(4)**, 350(2018), https://doi.org/10.1007/s13671-018-0234-9.
2. E. Apostolova, P. Lukova, A. Baldzhieva, P. Katsarov, M. Nikolova, I. Iliev, L. Peychev, B. Trica, F. Oancea, C. Delattre, and V. Kokova, *Polymers*, **12(10),** 2338(2020), https://doi.org/10.3390/polym12102338.
3. M. M. Damayanti and M. Rachmawati, *F1000Research*, **11(29)**, 29(2022), https://doi.org/10.12688/f1000research.74094.2.
4. E. Ö. Karagüzel, F. C. Arslan, E. K. Uysal, S. Demir, D. S. Aykut, M. Tat, and S. C. Karahan, *Comprehensive Psychiatry*, **89**, 61(2019), https://doi.org/10.1016/j.comppsych.2018.11.013.
5. H. Fukuoka, N. Fukuoka, Y. Daigo, E. Daigo, M. Ishikawa, and T. Kibe, *Photobiomodulation, Photomedicine, and Laser Surgery*, **39(9)**, 612(2021), https://doi.org/10.1089/photob.2020.4912.
6. T. Tanaka, and T. Kishimoto, *Cancer Immunology Research*, **2(4)**, 288(2014), https://doi.org/10.1158/2326-6066.CIR-14-0022.
7. B. Li, L. L. Jones, and T. L. Geiger, *The Journal of Immunology*, **201(10)**, 2934(2018), https://doi.org/10.4049/jimmunol.1800016.
8. M. Del Giudice, and S. W. Gangestad, *Brain, Behavior, and Immunity*, **70**, 61(2018), https://doi.org/10.1016/j.bbi.2018.02.013.
9. S. C. Jordan, J. Choi, I. Kim, G. Wu, M. Toyoda, B. Shin, and A. Vo, *Transplantation*, **101(1)**, 32(2017), https://doi.org/10.1097/TP.0000000000001452.
10. N. Błaszczyk, A. Rosiak, and J. Kałużna-Czaplińska, *Forests*, **12(5)**, 648(2021), https://doi.org/10.3390/f12050648.
11. R. Balamurugan, A. Stalin, A. Aravinthan, and J. H. Kim, *Medicinal Chemistry Research,* **24(1)**, 124(2015), https://doi.org/10.1007/s00044-014-1075-0.
12. M. A. Rauf, S. Zubair, and A. Azhar, *International Journal of Basic and Applied Sciences,* **4(2)**, 168 (2015), https://doi.org/10.14419/ijbas.v4i2.4123.
13. D. A. Tolmachev, O. S. Boyko, N. V. Lukasheva, H. Martinez-Seara, and M. Karttunen, *Journal of Chemical Theory and Computation,* **16(1)**, 677(2019), https://doi.org/10.1021/acs.jctc.9b00813.
14. A. W. Sousa Da Silva, and W. F. Vranken, *BMC Research Notes*, **5**, 367(2012), https://doi.org/10.1186/1756-0500-5-367.
15. H. Wang, X. Gao, and J. Fang, *Journal of Chemical Theory and Computation*, **12(11)**, 5596(2016), https://doi.org/10.1021/acs.jctc.6b00701.
16. R. Kumari, R. Kumar, and A. Lynn. *Journal of Chemical Information and Modeling*, **54(7)**, 1951(2014), https://doi.org/10.1021/ci500020m.
17. V. Triandafilidi, S. G. Hatzikiriakos, and J. Rottler, *Soft Matter*, **16(4)**, 1091(2020), https://doi.org/10.1039/C9SM02232E.
18. H. Li, D. Wang, Y. Yuan, and J. Min, *Arthritis Reseach and Therapy*, **19(1)**, 1(2017), https://doi.org/10.1186/s13075-017-1454-2.
19. J. Wang, and T. Hou, *Journal of Chemical Informat Modeling*, **52(5)**, 1199(2012), https://doi.org/10.1021/ci300064d.
20. D. R. Pomalingo, C. Suhandi, S. Megantara, and M. Muchtaridi, *Rasayan Journal of Chemistry,* **14(2)**, 698(2021), http://dx.doi.org/10.31788/ RJC.2021.1425770.
21. E. A. Rahim, *Rasayan Journal of Chemistry,* **14(4)**, 2529(2021), http://doi.org/10.31788/RJC.2021.1446471.
22. R. Marchiosi, W. D. dos Santos, R. P. Constantin, R. B. de Lima, A. R. Soares, A. Finger-Teixeira, T. R. Mota, D. M. de Oliveira, M. de Paiva Foletto-Felipe, J. Abrahão, and O. Ferrarese-Filho,

Phytochemistry Reviews, **19(4)**, 865(2020), https://doi.org/10.1007/s11101-020-09689-2.
23. Y. Tian, X. Cao, X. Li, H. Zhang, C. Sun, Y. Xu, W. Weng, W. Zhang, and R. Boulatov, *Journal of the American Chemical Society,* **142(43)**, 18687(2020), https://doi.org/10.1021/jacs.0c09220.
24. B. K. Tiwari, N. Brunton, and C. S. Brennan, *Wiley-Blackwell,* https://doi.org/10.1002/9781118464717
24. A. Stefanachi, F. Leonetti, L. Pisani, M. Catto, and A. Carotti, *Molecules* **23(2)**, 250(2018), https://doi.org/10.3390/molecules23020250.
25. S. Sakthi Priyadarsini, and P. R. Kumar, *Rasayan Journal of Chemistry,* **14(4)**, 2591(2021), http://dx.doi.org/10.31788/RJC.2021.1446529.
27. T. M. Fakih, *Pharmaceutical Sciences and Research,* **7(Special Issue on COVID-19)**, 65(2020), http://dx.doi.org/10.7454/psr.v7i4.1079.
28. A. Ibrar, S. A. Shehzadi, F. Saeed, and I. Khan, *Bioorganic&Medicinal Chemistry,* **26(13)**, 3731(2018), https://doi.org/10.1016/j.bmc.2018.05.042.
29. D. K. Mahapatra, S. K. Bharti, V. Asati, and S. K. Singh, *European Journal Medicinal Chemistry,* **174**, 142(2019), https://doi.org/10.1016/j.ejmech.2019.04.032.
30. M. Imran, A. Rauf, A. A. Khalil, S. Bawazeer, S. Patel, and Z. A. Shah, *Health Benefits of Secondary Phytocompounds from Plant and Marine Sources*, 81(Apple Academic Press, 2021).
31. S. L. Maiocchi, J. C. Morris, M. D. Rees, and S. R. Thomas, *Biochemical Pharmacology,* **135**, 90(2017), https://doi.org/10.1016/j.bcp.2017.03.016.
32. Z. Etwebi, G. Landesberg, K.Preston, S. Eguchi, and R. Scalia, *Hypertension*, **71**, 761(2018), https://doi.org/10.1161/HYPERTENSIONAHA.117.10305.

[RJC-8192/2022]